Biomimetic Electron Transfer Using Low Energy Excited States: A Green Perylene-Based Analogue of Chlorophyll *a*

Aaron S. Lukas, Yongyu Zhao, Scott E. Miller, and Michael R. Wasielewski*

Department of Chemistry and Center for Nanofabrication and Molecular Self-Assembly, Northwestern University, Evanston, Illinois 60208-3113

Received: November 8, 2001

We have prepared a green chromophore, 1,7-bis(pyrrolidin-1-yl)-3,4:9,10-perylene-bis(dicarboximide) (5PDI), that exhibits photophysical and redox properties similar to those of chlorophyll *a* (Chl *a*), yet unlike Chl *a*, it can be easily functionalized and incorporated into a wide variety of biomimetic electron donor−acceptor systems. The *N*,*N*′-dicyclohexyl derivative (5PDI) absorbs strongly ($\epsilon = 46\,000$ M^{-1} cm^{-1}) at 686 nm in toluene and fluoresces at 721 nm with a 35% quantum yield. Additionally, 5PDI is both oxidized and reduced in CH_2Cl_2 at 0.57 V and −0.76 V vs SCE, respectively, making it a facile electron donor or acceptor. Rodlike covalent electron donor−acceptor molecules 5PDI−PI, 5PDI−NI, and 5PDI−PDI were prepared by linking the imide group of the 5PDI donor to pyromellitimide (PI), 1,8:4,5-naphthalenebis(dicarboximide) (NI), and 1,7-bis(3,5-di-*tert*-butylphenoxy)-3,4:9,10-perylene-bis(dicarboximide) (PDI) acceptors via an N−N bond. Following femtosecond laser excitation of 5PDI, 5PDI−PI, 5PDI−NI, and 5PDI−PDI in both toluene and 2-methyltetrahydrofuran, the formation and decay of their excited and radical ion pair states were monitored directly by transient absorption spectroscopy. We also report steady state emission and spectro-electrochemistry data for these molecules, which aid in elucidation of the transient spectra and the mechanisms of photoinduced charge separation. In toluene, charge separation occurs with high yield only in 5PDI−NI and 5PDI−PDI, whereas for 5PDI−PI charge separation is slow relative to excited-state decay of ^{1*}5PDI−PI indicating that $\Delta G_{CS} \cong 0$. This fact provides a means of estimating the ionic radii of the photogenerated ions, which for perylene chromophores 5PDI and PDI are 7.6 ± 0.5 Å, whereas those of the PI and NI electron acceptors are 5.6 ± 0.5 Å. These ionic radii are used in turn to determine the free energies of reaction of the remaining molecules with the series. Electroabsorption measurements are used to show that the change in dipole moment, $\Delta\mu$ that occurs upon formation of ^{1*}5PDI is 3.5 D. The rates of charge separation in 5PDI−NI, 5PDI−PI, and 5PDI−PDI are compared to those of related donor−acceptor molecules having a 9-(pyrrolidin-1-yl)-perylene-3,4-dicarboximide (5PMI) donor. The 5PMI donor with $\Delta\mu = 15.4$ D has a lowest excited singlet state with significantly higher charge-transfer character than does 5PDI, and has greater electron density near the imide group to which the acceptor is attached. The rate constants for charge separation from ^{1*}5PMI are greater than those from ^{1*}5PDI, which suggests that the rates of electron transfer from donors with CT excited states to an attached acceptor depend on the charge distribution in the CT excited state.

Introduction

Donor−acceptor molecules designed to mimic photosynthetic charge separation and storage frequently employ porphyrin chromophores instead of the naturally occurring chlorophyll and bacteriochlorophyll molecules.[1] For the most part, this is a consequence of the simple fact that the synthesis of complex donor−acceptor molecules based on porphyrins is much easier. However, porphyrins fail to mimic the electronic asymmetries intrinsic to chlorins and bacteriochlorins in general.[2] Unlike porphyrins, these more highly reduced macrocycles possess strongly polarized optical transitions with significant extinction coefficients in the red and near-infrared regions of the optical spectrum, where a significant fraction of the solar spectrum occurs.[3] Exciton interactions between large transition dipoles of neighboring macrocycles result in spectrally shifted optical transitions that differentiate antenna from reaction center function.[4] In addition, metallochlorins and metallobacteriochlorins are generally easier to oxidize than the corresponding porphyrins.[5−7]

The synthesis of near-infrared (NIR) light absorbing and emitting organic chromophores for photochemical energy conversion and storage as well as optical data processing is an active area of research. Novel NIR absorbing chromophores[8] have been synthesized by extending the π-systems of push−pull aromatic molecules[9,10] or by employing organometallic compounds with $\pi-\pi^*$ electronic transitions.[11] Recently, improvements in the synthesis of terrylene[12] and quaterrylene[13,14] mono- and bis(dicarboximide)s, as well as the amidine−imides of perylene[15−18] have increased the use of these chromophores in spectroscopic studies. These chromophores offer broad spectral coverage in the NIR, large extinction coefficients, high fluorescence quantum yields, and are reversibly reduced at modest reduction potentials. For these reasons, they have been employed as chromophores in single molecule spectroscopic studies[19−23] and more recently as electron acceptors in multichromophoric arrays, which undergo efficient energy and electron-transfer reactions.[24,25]

On the other hand, the synthesis of easily oxidized species, which absorb in the red and NIR, has proven more challenging. The most commonly employed electron donors that absorb in

* To whom correspondence should be addressed. E-mail: wasielew@chem.northwestern.edu.

10.1021/jp014073w CCC: $22.00
Published on Web 01/19/2002

this spectral region are phthalocyanines,[26] chlorophylls, and bacteriochlorophylls.[27] However, the difficulty of synthesizing, or extracting and modifying these chromophores in large amounts, and in the case of the chlorins, their lack of long-term photostability has led us to consider alternative electron donor chromophores which absorb in this spectral region. Previous work from our laboratory has studied the effect of substituting a 3,4:9,10-perylenebis(dicarboximide) at the 1 and 7 positions with cyclic amines.[28] Electron donation from the amines into the perylene core produces a charge-transfer (CT) transition resulting in green compounds, which absorb in the spectral region between the bis(dicarboximide)s of terrylene (λ_{max}=665 nm) and quaterrylene (λ_{max}=760 nm).[29] This red shift in the absorption spectrum of 3,4:9,10-perylenebis(dicarboximide) by the addition of electron donating side groups and asymmetric extension of the aromatic core has been observed in other derivatives of 3,4:9,10-perylenebis(dicarboximide).[30] The electron donating ability of the cyclic amine substituents also introduces a large negative shift in the oxidation potentials of these macrocycles relative to 3,4:9,10-perylenebis(dicarboximide) without significantly affecting their reduction potentials. This makes these chromophores well suited for roles as either electron donor or acceptor moieties in intramolecular donor−acceptor (D−A) arrays. As an electron donor chromophore for use in biomimetic donor−acceptor arrays, these perylene compounds have the advantages of being relatively easy to synthesize, having strongly polarized optical transitions with large extinction coefficients, and being photochemically robust.

Our current work focuses on demonstrating the scope of photoinduced electron-transfer dynamics within a series of covalently linked D−A arrays that employ 1,7-bis(pyrrolidin-1-yl)-3,4:9,10-perylenebis(dicarboximide) (5PDI) as an electron donor. Donor−acceptor molecules 5PDI−PI, 5PDI−NI, and 5PDI−PDI were prepared by linking the imide group of the 5PDI donor to pyromellitimide (PI), 1,8:4,5-naphthalenebis-(dicarboximide) (NI), and 1,7-bis(3,5-di-*tert*-butylphenoxy)-3,4:9,10-perylenebis(dicarboximide) (PDI) acceptors via an N−N bond. The *N*,*N*′-dicyclohexyl derivative of the donor serves as a reference molecule. The D−A compounds as well as 5PDI are characterized using steady state and ultrafast spectroscopic techniques. The rates of charge separation (CS) in 5PDI−NI, 5PDI−PI, and 5PDI−PDI are compared to those of related donor−acceptor molecules having a 9-(pyrrolidin-1-yl)-perylene-3,4-dicarboximide (5PMI) donor. The ^{1*}5PMI state has significantly greater CT character than does ^{1*}5PDI, and has greater electron density near the imide group to which the acceptor is attached. The rate constants for charge separation from ^{1*}5PMI are larger than those from ^{1*}5PDI, which suggests that the rates of electron transfer from donors with CT excited states to an attached acceptor depend on the charge distribution in the CT excited state.

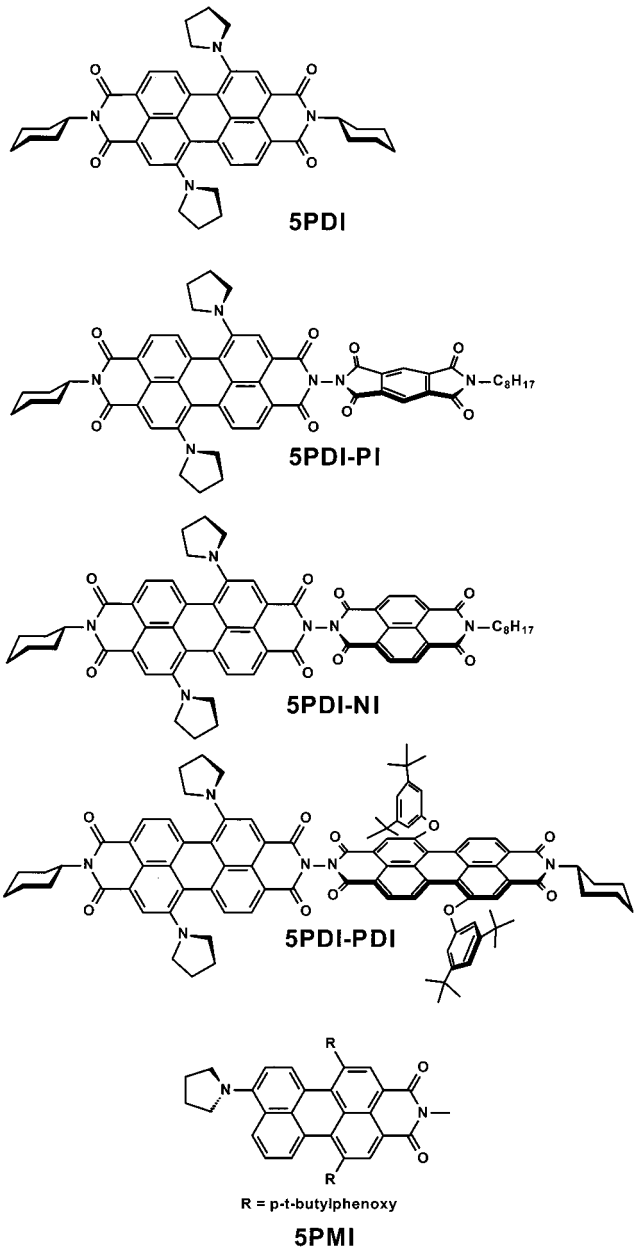

Experimental Section

The synthesis of 5PDI has been described previously,[28] whereas the syntheses of the donor−acceptor compounds 5PDI−PI, 5PDI−NI, and 5PDI−PDI are detailed in the Supporting Information. Briefly, the dyads were linked through N−N bonds at their imide groups via condensation of the monoanhydride of 5PDI, first with hydrazine monohydrate, followed by condensation of the resulting aminoimide with the appropriate monoanhydrides of the electron acceptor groups. Characterization was performed with a Varian 400 MHz NMR spectrometer and Perseptive BioSystems time-of-flight MALDI mass spectrometer.

Femtosecond transient absorption measurements were made using a regeneratively amplified titanium sapphire laser system operating at a 2 kHz repetition rate.[31] The frequency-doubled output from the laser was used to provide 420 nm, 130 fs pulses for excitation, whereas 530 and 680 nm, 130 fs excitation pulses were produced using an optical parametric amplifier.[32] A white light continuum probe pulse was generated by focusing the 840 nm fundamental into a 1 mm sapphire disk. Cuvettes with a 2 mm path length were used and the samples were irradiated with 0.5 μJ per pulse focused to a 200 μm spot. The optical density at the excitation wavelength was typically 0.3−0.5. The samples were stirred during the experiment using a wire stirrer to prevent thermal lensing and sample degradation. The total instrument response for the pump−probe experiments was 180 fs. Steady-state absorption and emission spectra were performed on a Shimadzu 1601 UV/Vis spectrophotometer and PTI instruments single photon counting fluorimeter, respectively. A 10 mm quartz cuvette was used with optical density at 625 nm maintained at 0.1 ± 0.05 A. U. to avoid reabsorption artifacts. All solvents were spectrophotometric grade. 2-Methyltetrahydrofuran (Aldrich) was distilled immediately prior to use.

TABLE 1: Steady State Properties of Compounds

	toluene				MTHF			
compd	λ_{Abs}	λ_{Em}	E_S	Φ_F	λ_{Abs}	λ_{Em}	E_S	Φ_F
5PDI	686	721	1.77	0.35	683	733	1.76	0.28
5PDI−PI	696	740	1.73	0.21	697	745	1.73	0.01
5PDI−NI	696	735	1.73	0.01	696	744	1.73	<0.001
5PDI−PDI	695	742	1.74	0.13	695	742	1.73	<0.001

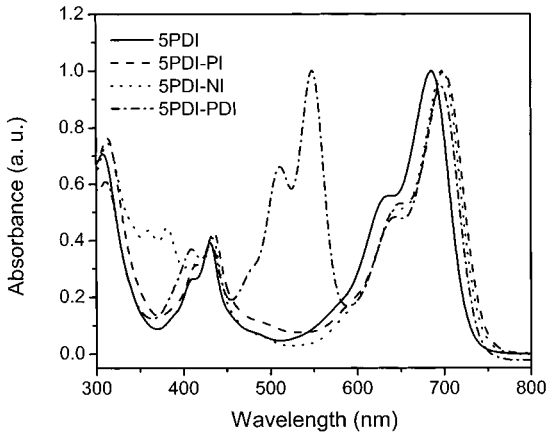

Figure 1. Ground-state absorption spectra of the indicated compounds in toluene.

Kinetic analyses were performed at several wavelengths using a nonlinear least-squares fit to either a general sum-of-exponentials function or to a series A → B → C kinetic mechanism using the Levenberg−Marquardt algorithm. The wavelengths targeted in these analyses center on the relatively narrow absorbances of NI^-, PI^-, and PDI^-. Spectral overlap of these well-separated absorption bands with those of ^{1*}5PDI is sufficiently small at numerous wavelengths within the NI^-, PI^-, and PDI^- bands to permit a self-consistent set of time constants to be determined.[33]

Electrochemical measurements were performed using a CH Instruments Model 622 electrochemical workstation. The solvents were butyronitrile (PrCN) and methylene chloride containing 0.1 M tetra-*n*-butylammonium perchlorate electrolyte. A 1.0 mm diameter platinum disk electrode, platinum wire counter electrode, and Ag/Ag_xO reference electrode were employed. The ferrocene/ferrocinium (Fc/Fc^+, 0.52 vs SCE) was used as an internal reference for all measurements.

Electroabsorption experiments were performed in 100 μm path length cells in a frozen MTHF matrix at 77 K. Typical root-mean-square electric field strengths (220 Hz) were 3.4×10^5 V cm^{-1}. Additional details concerning the experimental apparatus and data analysis can be found in the references.[34,35]

Results and Discussion

Steady-State Spectroscopy. The absorption and emission maxima of 5PDI in both toluene and MTHF are listed in Table 1, and its electronic absorption spectrum in toluene is shown in Figure 1. The presence of the amine substituents in the bay (1 and 7) positions of the 3,4:9,10-perylenebis(dicarboximide) introduces an intense ($\epsilon = 46\,000$ M^{-1} cm^{-1}), broad absorption, which is significantly red shifted (138 nm) relative to that of the corresponding 1,7-bis(phenoxy) derivatives of 3,4:9,10-perylenebis(dicarboximide).[16] The solvent dependent Stokes shifts and emission quantum yields of this band strongly suggest that the lowest excited state has charge transfer (CT) character. The lowest energy optical transitions in each compound belong to the 5PDI chromophore. Replacement of one of the *N*-cyclohexyl substituents of 5PDI by an imide-imide linkage to the acceptor red shifts the absorption and emission maxima of the 5PDI chromophore by 10 nm. This is due to the electron withdrawing inductive nature of the imide substituent relative to the cyclohexyl group and has been observed in analogous compounds.[36] Thus, ^{1*}5PDI is stabilized by 0.03 to 0.04 eV within the donor−acceptor molecules relative to ^{1*}5PDI, Table 1. All the excited state energies are approximately 1.73 eV, which compares favorably with the 1.86 eV lowest excited singlet state energy of chlorophyll *a* (Chl *a*).[3]

TABLE 2: Redox Potentials of Compounds in PrCN (V vs SCE)

compd	E_{5PDI}^{+1}	E_{5PDI}^{+2}	E_{5PDI}^{-1}	E_{5PDI}^{-2}	E_{ACC}^{+1}	E_{ACC}^{-1}
5PDI	0.68	0.75	−0.76	−0.94		
5PDI−PI	0.74	0.81	−0.62	−0.84	>2.0	−0.72
5PDI−NI	0.74	0.82	−0.71	−0.87	>2.0	−0.40
5PDI−PDI	0.75	0.82	−0.70	−0.89	>2.0	−0.47

The fluorescence quantum yield of 5PDI was determined relative to 5PMI ($\Phi_{F,5PMI} = 0.48$ in toluene and 0.38 in MTHF[36]). In toluene and MTHF, the quantum yield of 5PDI is 0.35 and 0.28, respectively. The moderately high fluorescence quantum yield of 5PDI compares favorably with the 0.35 yield for Chl *a*.[3] The emission from the 5PDI chromophore is quenched significantly by the attachment of electron acceptor groups, Table 1. The only exception is 5PDI−PI in toluene, which has a fluorescence quantum yield that is about one-third smaller than that of 5PDI, indicating that the rate of CS within ^{1*}5PDI−PI may be similar to the rate of excited-state decay of ^{1*}5PDI. The fluorescence quantum yields of 5PDI−NI and 5PDI−PDI in toluene are much lower. In MTHF all the donor−acceptor compounds display significant excited-state quenching, where once again emission from 5PDI−NI and 5PDI−PDI is quenched most strongly.

Electrochemistry and Spectroelectrochemistry. The electrochemical properties of aromatic imides and diimides are highly sensitive to the nature of the imide substituent.[37] Imides substituted with electron withdrawing groups have more positive reduction potentials due to inductive stabilization of the anion radical. Cyclic voltammetry conducted in PrCN containing 0.1 M tetra-*n*-butylammonium perchlorate confirms that the local environment plays a significant role in determining both the oxidation and reduction potentials of the 5PDI donor chromophore, as well as the acceptors attached to it, Table 2. At negative potentials 5PDI exhibits two reversible waves spaced by approximately 300 mV, similar to those of previously reported 3,4:9,10-perylenebis(dicarboximide)s.[29] Both the first and the second reduction potentials of 5PDI are shifted to more positive potentials by approximately 0.1 V for 5PDI−PI, 5PDI−NI, and 5PDI−PDI, wherein it is directly linked to the electron acceptors via an imide-imide bond. At more positive potentials, two overlapping oxidation waves corresponding to reversible formation of the singly and doubly oxidized species are observed. Again, substitution of 5PDI with imide groups in the donor−acceptor compounds positively shifts its oxidation potentials, making 5PDI more difficult to oxidize by approximately 0.1 V within the donor−acceptor compounds.

The steady state ground electronic absorption spectrum of the singly oxidized state of 5PDI in methylene chloride is displayed in Figure 2. Although the first and second oxidation waves in PrCN occur at 0.68 and 0.75 V vs SCE, these shift to 0.55 and 0.87 V vs SCE in methylene chloride, so that it is relatively easy to control the bulk oxidation of 5PDI in methylene chloride to yield only $5PDI^+$. The $5PDI^+$ cation radical exhibits peaks at 410, 550, 880, and 1020 nm, whereas

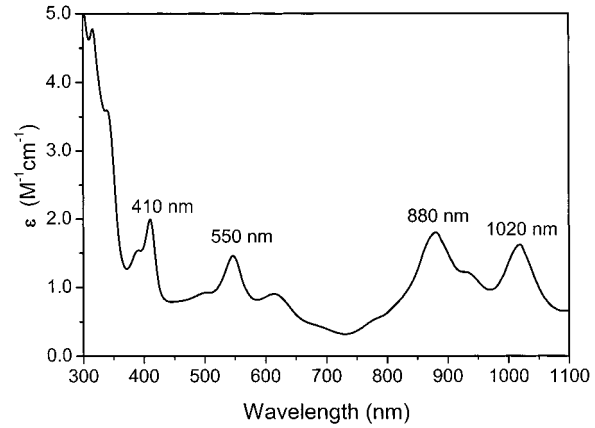

Figure 2. Electrochemically generated ground-state spectrum of the $5PDI^+$ in CH_2Cl_2.

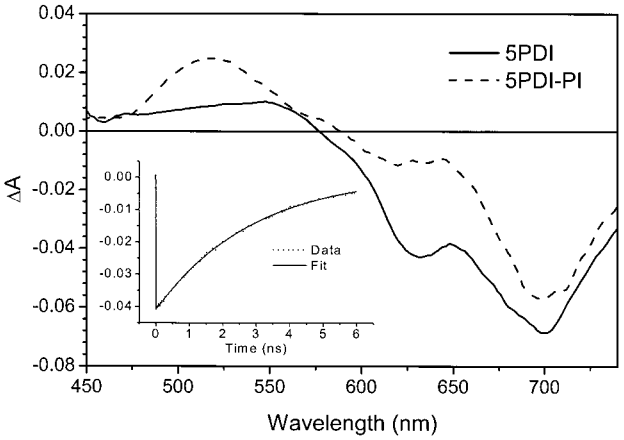

Figure 3. Transient absorption spectra of the indicated compounds in toluene at $\tau = 500$ ps following excitation with a 420 nm, 130 fs laser flash. Inset: Transient absorption kinetics monitoring changes in ΔA at 700 nm with the associated fits to the data.

its doubly oxidized species (not shown) exhibits broad peaks at 610, 490, and 410 nm. The extinction coefficient of the 880 nm band of $5PDI^+$ is 17 400 M^{-1} cm^{-1}, and is substantially larger than that of the 820 nm band ($\epsilon = 6700$ M^{-1} cm^{-1}) of the Chl *a* cation radical.[38] Elucidation of the ground electronic spectrum of $5PDI^+$ will aid in identifying this ion in transient absorption spectra arising from photoinduced electron transfer in the donor−acceptor compounds.

Time-Resolved Spectroscopy. Excitation of 5PDI with 420 nm, 130 fs laser pulses yields ^{1*}5PDI within the 180 fs instrument function of the apparatus. The resulting transient absorption spectrum in toluene at 500 ps after the laser flash is shown in Figure 3. The major feature centered at 700 nm is bleaching of the ground-state absorption, while ^{1*}5PDI has a small positive absorption feature that extends from 450 to 570 nm. The bleach is red shifted somewhat from the 686 absorption maximum of the ground state by its convolution with stimulated emission from ^{1*}5PDI. The excited-state lifetimes of ^{1*}5PDI are $\tau = 4.5$ ns and $\tau = 3.0$ ns, in toluene and MTHF, respectively, as determined by the recovery of the ground-state bleaches at 625 and 700 nm. In addition to its CT absorption at 686 nm, 5PDI retains a higher energy $\pi-\pi^*$ transition centered at 435 nm, which is likely due to formation of the ^{1**}5PDI second excited singlet state. Excitation of 5PDI directly into its 686 nm CT transition with 680 nm, 130 fs laser flashes results in transient absorption spectra and kinetics that are identical to those observed when 5PDI is excited with 420 nm pulses, indicating that rapid internal conversion occurs to form the CT excited state within the 180 fs instrument response.

TABLE 3: Free Energies and Time Constants for CS and CR

	ΔG_{CS} (eV)	τ_{CS} (ps)	ΔG_{CR} (eV)	τ_{CR} (ps)
		Toluene		
5PDI−PI	0.00	8100	−1.73	
5PDI−NI	−0.32	40	−1.41	550
5PDI−PDI	−0.29	50	−1.45	2000
		MTHF		
5PDI−PI	−0.24	50	−1.49	370
5PDI−NI	−0.56	6	−1.17	13
5PDI−PDI	−0.49	13	−1.24	300

Attachment of the PI electron acceptor to 5PDI within 5PDI−PI provides an electron transfer pathway that can potentially deactivate the ^{1*}5PDI excited state. The transient absorption spectrum of ^{1*}5PDI−PI in toluene at 500 ps following the laser flash, Figure 3, shows a somewhat smaller bleach at 700 nm than does ^{1*}5PDI, whereas the 2.9 ns time constant for the decay of ^{1*}5PDI−PI is slightly smaller than the corresponding 4.5 ns time constant for ^{1*}5PDI, inset to Figure 3. The well-characterized spectrum of the PI^- anion radical has a sharp absorption at 715−730 nm ($\epsilon = 41\,700$ M^{-1} cm^{-1}).[39] The decrease in the magnitude of the bleach at 700 nm in 5PDI−PI relative to that of 5PDI may be due to formation of a small amount of $5PDI^+-PI^-$ in which the positive absorption of PI^- cancels part of the overall bleach at 700 nm. In addition, the spectrum of 5PDI−PI in Figure 3 has a broad feature at 500−550 nm. This absorption is similar to the spectral features observed for $5PDI^+$ in Figure 2. These facts support the idea that the transient spectrum at 500 ps following excitation of 5PDI−PI is consistent with formation of a low yield of $5PDI^+-PI^-$ in toluene. Assuming that electron transfer is the only additional decay pathway of ^{1*}5PDI that is competitive with its intrinsic decay, the quantum yield of electron transfer is $\varphi_{ET} = 1 - (\tau_X/\tau_0) = 0.35$, where τ_X and τ_0 are the excited-state decay time constants for ^{1*}5PDI−PI and ^{1*}5PDI, respectively. Taken together these data strongly suggest that $\Delta G \cong 0$ for the reaction ^{1*}5PDI−PI $\rightarrow$ $5PDI^+-PI^-$ in toluene. Increasing the solvent polarity by using MTHF results in a dramatic decrease in the time constant of CS, Table 3, which is expected, if ΔG for the electron-transfer reaction becomes negative.

The NI electron acceptor within 5PDI−NI is the easiest to reduce of the three electron acceptors used in these studies. The fluorescence quantum yields of 5PDI−NI in toluene and MTHF indicate that the ^{1*}5PDI−NI excited-state undergoes very fast nonradiative decay. This dark decay process is confirmed to be photoinduced CS by the transient absorption spectra shown in Figure 4. In addition to the ground-state bleach of 5PDI, again centered near 700 nm, the spectra exhibit peaks at 470 and 605 nm arising from the NI^- anion radical ($\epsilon = 26000$ M^{-1} cm^{-1}).[37] The kinetics monitored at the 470 nm peak in both toluene and MTHF are shown in the inset to Figure 4. Absorption features due to both ^{1*}5PDI and $5PDI^+$ are also observed as a shoulder on the red side of the 470 nm NI^- peak. The time constants for CS and CR listed within Table 3 again show that the rates for both processes increase dramatically upon increasing the solvent polarity in going from toluene to MTHF.

5PDI−PDI is a donor−acceptor molecule comprised entirely of chromophores that are 3,4:9,10-perylenebis(dicarboximide) derivatives. The electron-accepting PDI chromophore is functionalized with 3,5-di-*tert*-butylphenoxy groups, which increase its solubility and result in only small perturbations of the ground absorption spectrum and electrochemical properties relative to

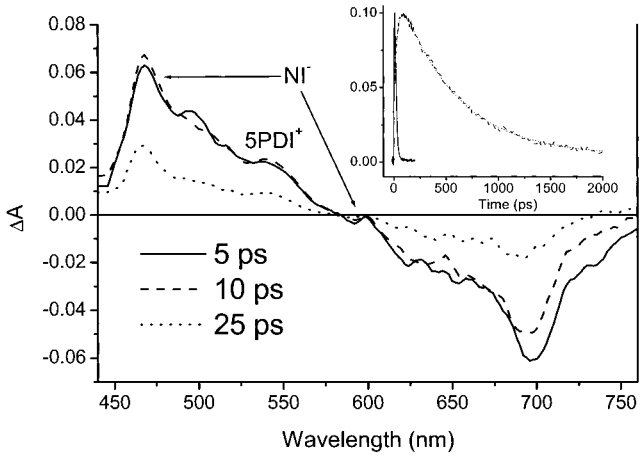

Figure 4. Transient absorption spectra of 5PDI−NI in MTHF at the indicated times following excitation with a 420 nm, 130 fs laser flash. Inset: Kinetics monitoring the rise and decay of the 470 nm absorption arising from the NI^- anion radical in toluene (- - - -) and MTHF (−) with the associated fits to the data.

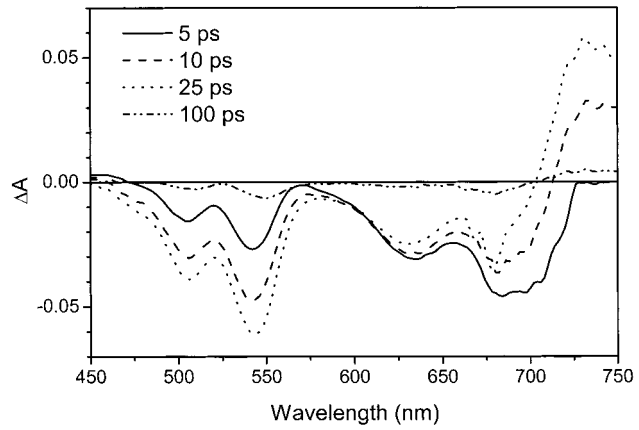

Figure 5. Transient absorption spectra of 5PDI−PDI in toluene at the times indicated following excitation with a 420 nm, 130 fs laser flash.

3,4:9,10-perylenebis(dicarboximide) unsubstituted at the 1 and 7 positions. Excitation of 5PDI−PDI with 680 nm, 130 fs laser pulses results in formation of the $5PDI^+-PDI^-$ ion pair in both toluene and MTHF with time constants for CS and CR listed in Table 3. Transient absorption spectra of 5PDI−PDI in MTHF are shown in Figure 5. The negative absorption changes at 510 and 550 nm arise from depletion of the PDI acceptor ground state upon formation of the ion pair. Negative absorption changes are also observed at 630 and 690 nm from ground-state bleaching of 5PDI. The large absorption at 730 nm is due to the PDI^- anion radical ($\epsilon = 74200\ M^{-1}\ cm^{-1}$).[40,41] Kinetics monitoring the rise and decay of the 510, 550, and 730 nm bands give similar time constants for CS and CR in both toluene and MTHF. Furthermore, excitation of 5PDI−PDI with either 420 or 530 nm, 130 fs laser pulses result in identical time constants for CS, indicating that the $5PDI-{}^{1*}PDI \rightarrow {}^{1*}5PDI-PDI$ energy transfer occurs with a time constant that is less than the 180 fs instrument response.

Ground and Excited-State Structures. The energy-minimized ground-state structure of the 5PDI chromophore with hydrogen atoms attached to the imide nitrogen atoms determined by semiempirical molecular orbital calculations using the PM3 method[42,43] is displayed in Figure 6A. The figure displays an end-on view of the molecule in which all of the hydrogen atoms have been removed for clarity. This view shows the distortion

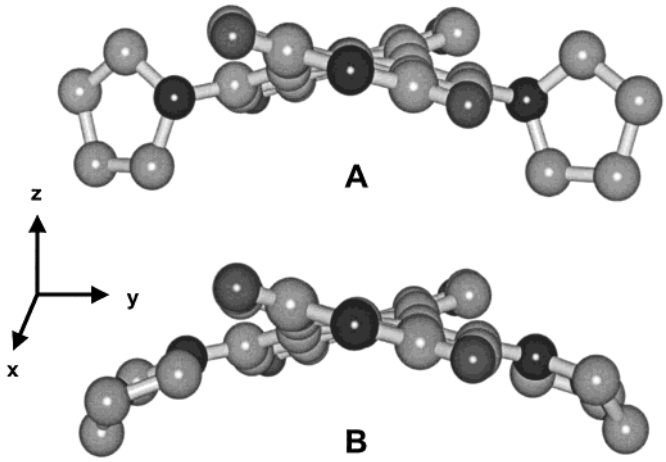

Figure 6. (A) Energy-minimized PM3 structure of 5PDI. (B) Energy-minimized ZINDO/S structure of ^{1*}5PDI.

TABLE 4: Calculated Ground and Excited State Properties of 5PDI and 5PMI

	μ_x	μ_y	μ_z	μ
5PDI				
S_0 dipole moment (0 cm^{-1})[a]	0.08	−0.03	0.45	0.5
S_1 dipole moment (14186 cm^{-1}, 705 nm)[b]	0.1	0.7	3.1	3.2
$S_0 \rightarrow S_1$ transition moment[b]	9.1	3.3	−1.1	9.7
5PMI				
S_0 dipole moment (0 cm^{-1})[a]	5.2	−1.0	0.6	5.3
S_1 dipole moment (18869 cm^{-1}, 530 nm)[b]	15.4	−1.7	1.8	15.6
$S_0 \rightarrow S_1$ transition moment[b]	10.8	−0.2	1.2	10.9

[a] Energy-minimized PM3 structure. [b] Energy-minimized ZINDO/S structure with CI (99 configurations).

of the aromatic core created by the presence of the two pyrrolidine rings, as their 1,7 substitution pattern results in both rings being pushed out of the aromatic plane in the same direction. The resulting dihedral angle between the 1,12 and 6,7 positions is 24°, which introduces an overall asymmetry into the molecule. The ground-state dipole moment of 0.5 D is oriented perpendicular to the average plane of the aromatic core of the molecule, Table 4.

The energy-minimized structure of the lowest excited singlet state of 5PDI determined by the ZINDO/S method[44] using configuration interaction involving 99 configurations is shown in Figure 6B. The PM3 ground-state structure was used as a starting point for the calculation. A comparison of the two structures in Figure 6 shows that excitation of 5PDI results in rotation of the two pyrrolidine rings into the plane of the perylene core accompanied by an overall flattening of the geometry around the pyrrolidine nitrogen atoms. This results in charge transfer from the pyrrolidine nitrogen lone pairs into the perylene π system as a consequence of increased overlap between them. The calculated excited-state energy is 14 186 cm^{-1} or 1.76 eV, Table 3, which agrees remarkably well with the measured excited-state energy of 5PDI. In addition, the calculated value of $\Delta\mu = 2.7$ D agrees well with the measured value of 3.5 D, which was obtained by modeling the electroabsorption spectrum of 5PDI shown in Figure 7 using methods described earlier.[34,35] The close quantitative agreement between the calculations and experimental values is most likely fortuitous, given the approximate nature of the ZINDO/S method used to calculate the excited-state properties of 5PDI. Nevertheless, the qualitative features of the calculations can be used to understand the changes in the 5PDI electronic structure that occur upon excitation.

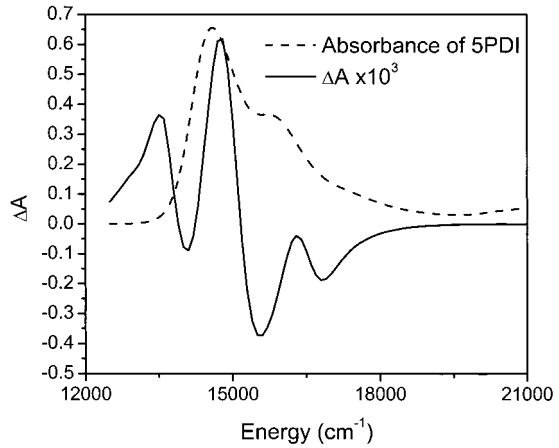

Figure 7. Electroabsorption spectrum of 5PDI in MTHF at 77K using an applied voltage of 3.4×10^5 V cm^{-1} at 220 Hz (−). The spectrum is compared with the absorption spectrum of 5PDI (- - - -).

The calculated vector components of both the ground and excited state dipole moments of 5PDI show that charge is primarily transferred in a direction perpendicular to the plane of the perylene core, Table 4. This is consistent with charge transfer from the pyrrolidine nitrogen atoms to the perylene core, given the distortion from planarity of the perylene core along the *z*-axis, Figure 6. However, if one neglects the pyrrolidines, the perylene core remains symmetric to rotation about its *y*-axis, and charge delocalized within it is symmetrically displaced toward both electronegative imide groups resulting in a small change in $\Delta\mu$. The calculated transition moment for the $S_0 \rightarrow S_1$ transition is strongly polarized in the plane of the perylene along the *x*-axis of the molecule. This result supports the idea that excitation of 5PDI results in charge redistribution along the perylene *x*-axis toward the symmetrically placed imide groups. The steady-state absorption and emission spectra of all the donor−acceptor molecules show that the addition of electron withdrawing groups at the imides accentuates this delocalization in both the ground and the excited states of 5PDI. The fact that the change in state dipole moment, $\Delta\mu$ and the $S_0 \rightarrow S_1$ transition moment are perpendicular in 5PDI is not unusual, and has been observed in other dye molecules.[45]

PM3 calculations were also performed on the donor−acceptor molecules to obtain their energy-minimized ground-state structures. The center-to-center donor−acceptor distances, r_{DA}, within 5PDI−PI and 5PDI−NI are both 10.4 Å, whereas r_{DA} increases to 12.4 Å in 5PDI−PDI. The principal degrees of conformational freedom in these donor−acceptor compounds are restricted rotations about the N−N bonds of the imides. Steric hindrance between the carbonyl oxygen atoms on adjacent imide groups severely limits rotations about this axis, and positions the aromatic planes of the chromophores nearly orthogonal to one another. The energy-minimized structures yield dihedral angles between 72° and 87° between the planes defined by the imide groups of 5PDI and those of the acceptors. This results in relatively weak electronic coupling between 5PDI and the electron acceptors.

Charge Separation and Recombination Energetics. An accurate assessment of the free energies of the ion pairs, ΔG_{IP}, is important for understanding the photophysics observed within these donor−acceptor molecules, and can be particularly difficult in low polarity media such as toluene. The free energies of the ion pairs in low polarity solvents are frequently calculated using an expression derived by Weller based on the Born dielectric continuum model that employs the redox potentials of the donor and acceptor determined in a polar solvent along with the Born solvation energies of both ions in the low polarity solvent of interest, eq 1[46]

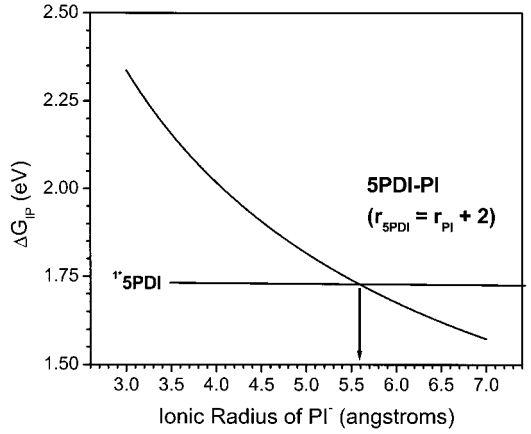

Figure 8. Dependence on the free energy (ΔG_{IP}) of $5PDI^+-PI^-$ assuming that $\Delta G_{IP} \cong E_S$ and $r_{5PDI} = r_{PI} + 2$ Å using eq 1.

$$\Delta G_{IP} = E_{OX} - E_{RED} - \frac{e^2}{r_{DA}\epsilon_S} + e^2\left(\frac{1}{2r_{5PDI}} + \frac{1}{2r_A}\right)\left(\frac{1}{\epsilon_S} - \frac{1}{\epsilon_{SP}}\right) \quad (1)$$

where E_{OX} and E_{RED} are the oxidation and reduction potentials of the donor and acceptor, *e* is the charge of the electron, r_{DA} is the ion pair distance, r_{5PDI} and r_A are the ionic radii of 5PDI and the acceptor, respectively, ϵ_S is the static dielectric constant of the low polarity solvent of interest, and ϵ_{SP} is the static dielectric constant of the high polarity solvent in which the redox potentials are determined. Apart from the shortcomings intrinsic to the use of simple continuum models of solvation, inaccuracies within this treatment arise mainly from difficulties in estimating the ionic radii of the donor and acceptor, as well as the omission of terms due to higher order multipoles present in low polarity solvents such as toluene, which can further stabilize the ion pair. Previous work by Zimmt and Waldeck has shown that in toluene there is little stabilization of intramolecular ion pairs by the inclusion of higher order dipole−dipole or dipole−quadrupole terms.[47] They have shown that for toluene continuum models err by less than 0.01 eV in the estimation of ΔG_{IP}, when higher order multipole terms are excluded. Therefore, if ΔG_{IP} can be obtained by independent means for a reference donor−acceptor molecule, then eq 1 can be can be used to obtain the effective radii of the ions. Using these ionic radii, eq 1 can then be used to calculate ΔG_{IP} for the entire series of structurally related donor−acceptor molecules.

The energy-minimized PM3 structures of each donor−acceptor molecule show that the N−N distances within the PI (6.8 Å) and NI (7.1 Å) acceptors are approximately the same, as well as about 4 Å smaller than the N−N distances within 5PDI (11.2 Å) and PDI (11.2 Å), so that the ionic radii of PI and NI should be nearly the same, as should those of 5PDI and PDI. Thus, if we assume that $\Delta G_{IP} \cong E_S$ for $5PDI^+-PI^-$ in toluene, and that $r_{5PDI} = r_{PI} + 2$ Å, plotting ΔG_{IP} as a function of r_{PI} using eq 1 gives $r_{PI} = 5.6$ Å for 5PDI−PI, Figure 8, which in turn implies that $r_{5PDI} = 7.6$ Å. In concert with recent theoretical studies, these results suggest that an accurate assessment of ΔG_{IP} using continuum theory must include some contribution of solvent molecules to the effective ionic radii, and that inaccuracies in ΔG_{IP} arise from underestimation of the ionic radii in low polarity solvents.[48−50] Using $r_{PI} = r_{NI} = 5.6$ Å and $r_{5PDI} = r_{PDI} = 7.6$ Å, eq 1 was used to calculate ΔG_{IP} for each donor−acceptor molecule in both toluene and MTHF.

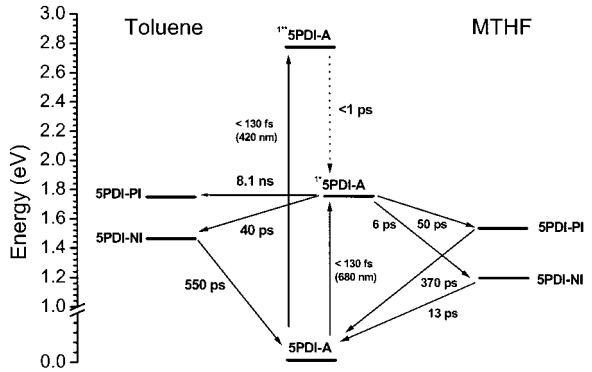

Figure 9. Energy level diagram for 5PDI−PI and 5PDI−NI in toluene and MTHF.

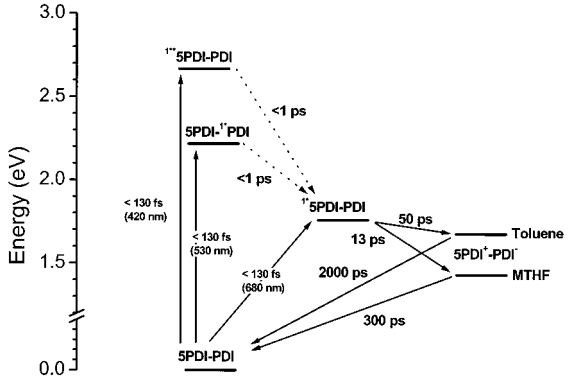

Figure 10. Energy level diagram for 5PDI−PDI in toluene and MTHF.

Table 3 lists the free energies for CS and CR determined from ΔG_{IP} using eqs 2 and 3

$$\Delta G_{CS} = \Delta G_{IP} - E_S \quad (2)$$

$$\Delta G_{CR} = -\Delta G_{IP} \quad (3)$$

These data show that charge separation is thermodynamically favorable for all the donor−acceptor molecules in both toluene and MTHF, except for 5PDI−PI in toluene, which is used to calibrate the energy scale. These results agree well with the experimental observations. Taken in their entirety, the rates for CS within these donor−acceptor molecules increase as ΔG_{CS} becomes increasingly negative, while the rates of CR increase as ΔG_{CR} becomes more positive. This behavior indicates that CS occurs in the normal region of the Marcus rate vs free energy profile, whereas CR is an inverted region process.[51] The electron-transfer pathways and time constants for CS and CR as well as the energies of the excited and ion pair states for 5PDI−PI and 5PDI−NI in toluene and MTHF are summarized in Figure 9, whereas those for 5PDI−PDI are shown in Figure 10.

Ultrafast Charge Separation and Excited-State Charge Distributions. It has been proposed that the primary dimeric electron donor within the photosynthetic reaction center exhibits a charge resonance interaction between the chlorophylls of the dimer that may facilitate the subsequent charge separation reaction.[52−54] Nevertheless, electron-transfer reactions in chemical systems that are initiated from singlet charge transfer (CT) states localized on the donor or the acceptor have not been studied extensively.[55,56] It is useful to compare the time constants for CS in 5PDI−PI and 5PDI−NI with those of related donor−acceptor molecules that also have CT excited states as well as similar linkages between the imide groups of the donor and the acceptor. We have reported CS and CR time constants for the corresponding 5PMI donors linked to both PI and NI acceptors.[36] A gauge of the redistribution of charge that occurs when a chromophore is excited can be made by examining the difference between the ground and excited-state dipole moments of the chromophore, $\Delta\mu$. The value of $\Delta\mu = 3.5$ D obtained from the electroabsorption spectrum of 5PDI is about 4.5 times smaller that observed for 5PMI, where $\Delta\mu = 15.4$ D.[36] The calculated value of $\Delta\mu = 10.3$ D for 5PMI, Table 4, is in reasonably good agreement with the experimental value given the approximate nature of the excited-state calculations. The dipole moments for both S_0 and S_1 of 5PMI are dominated by their *x* components that lie along the long axis of the perylene core. In addition, the transition moment for 5PMI is strongly polarized along the *x* direction. The most obvious difference between the structures of the perylene cores within PMI and PDI is the presence of one and two imides, respectively, which makes the perylene core of 5PMI asymmetric, while that of 5PDI is symmetric. The values of $\Delta\mu$ for PMI and PDI strongly suggest that excitation of these molecules results in a greater redistribution of negative charge toward the single imide group in PMI than toward the two imide groups in PDI. As a consequence, charge transfer to a PI or NI acceptor attached to the imide of ^{1*}5PMI should occur at a shorter effective distance than is the case for the much more symmetric charge distribution in the ^{1*}5PDI donor. This decrease in the effective distance over which the electron is transferred should result in an increase in overall electronic coupling between the donor and the acceptor that in turn should translate into a faster CS rate, if other parameters, such as the free energies of reaction, are similar.

TABLE 5: Free Energies and Time Constants for CS and CR

	ΔG_{CS} (eV)	τ_{CS} (ps)	ΔG_{CR} (eV)	τ_{CR} (ps)
		Toluene		
5PMI−PI	−0.15	64	−1.73	800
5PMI−NI	−0.36	7.0	−1.54	147
		MTHF		
5PMI−PI	−0.21	2.1	−1.63	8.8
5PMI−NI	−0.42	2.4	−1.44	3.0

The free energies of reaction and the time constants for CS and CR for 5PMI−PI and 5PMI−NI are given in Table 5. Comparing 5PMI−PI with 5PDI−PI in toluene, the difference in ΔG_{CS} is only 0.15 eV for these two molecules, yet the rate of CS for 5PMI−PI is more than 100 times greater than that of 5PDI−PI. For the same molecules in MTHF, where the difference in ΔG_{CS} is only 0.03 eV, the rate of CS for 5PMI−PI remains 25 times greater than that of 5PDI−PI. The same trend occurs for the molecules with NI acceptors. Comparing 5PMI−NI with 5PDI−NI in toluene, the difference in ΔG_{CS} is only 0.04 eV, yet the rate of CS for 5PMI−PI is nearly 7 times greater than that of 5PDI−NI. For the same molecules in MTHF, where the difference in ΔG_{CS} is 0.14 eV, the rate of CS for 5PMI−NI is still 3 times greater than that of 5PDI−NI. In all of these comparisons, the trend is in the same direction, which suggests that electron donors having more strongly dipolar excited states, where the dipole direction results in accumulation of negative charge close to the electron acceptor, have enhanced rates of charge separation.

Steady state and time resolved measurements confirm unambiguously that CS in 5PDI−PDI occurs in both toluene and MTHF from the CT lowest excited state of 5PDI, accessed directly via excitation with 680 nm light. Excitation of 5PDI−PDI with either 420 or 530 nm light results in identical steady-state quantum yields and time constants for CS and CR. This

suggests that both ^{1**}5PDI−PDI → ^{1*}5PDI−PDI internal conversion and 5PDI-^{1*}PDI → ^{1*}5PDI−PDI energy transfer occur with near unity yields, and that each process occurs with $\tau < 1$ ps. The ultrafast nature of the energy transfer process within 5PDI−PDI is not surprising, as the emission from ^{1*}PDI overlaps strongly with the absorption of 5PDI, as is required for Förster transfer. In addition, the single covalent bond between 5PDI and PDI should allow for rapid energy transfer via the exchange (Dexter) mechanism.

Conclusions

The 5PDI chromophore provides a functional biomimetic alternative to the use of Chl *a* in donor−acceptor systems. On the basis of the rates of electron transfer, the presence of a CT lowest excited-state promotes CS within these compounds when sufficient driving force is present. The observation that $\Delta G_{CS} \cong E_S$ for $5PDI^+-PI^-$ in toluene is used to determine the effective ionic radii of the ions in this series of donor−acceptor molecules, and the free energies of CS and CR in both toluene and MTHF. A comparison of the 5PDI chromophore with 5PMI shows that redistribution of negative charge in the direction of the attached electron acceptor serves to make the donor−acceptor distance effectively smaller, thereby increasing the rate of charge separation. Further work is also underway to employ the electron donating and accepting properties of 5PDI in tandem for the construction of large self-assembling multichromophoric arrays that use low energy photons for photochemical energy conversion and storage.

Acknowledgment. The authors wish to thank Dr. David Gosztola (Argonne National Laboratory) for obtaining the spectrum in Figure 2, and Mr. Robert C. Johnson and Prof. Joseph T. Hupp (Northwestern) for performing the electroabsorption measurements on 5PDI. This work was supported by the Division of Chemical Sciences, Office of Basic Energy Sciences, U.S. Department of Energy under Grant No. DE-FG02-99ER14999.

Supporting Information Available: Synthetic and spectroscopic details (PDF). This material is available free of charge via the Internet at http://www.pubs.acs.org.

References and Notes

(1) Gust, D.; Moore, T. A.; Moore, A. L. *Acc. Chem. Res.* **2001**, *34*, 40−48.
(2) Wasielewski, M. R. In *Chlorophylls*; Scheer, H., Ed.; CRC: Boca Raton, 1991; pp 269−286.
(3) Goedheer, J. C. In *The Chlorophylls*; Vernon, L. P., Seely, G. R., Eds.; Academic Press: New York, 1966; pp 147−184.
(4) Katz, J. J.; Norris, J. R.; Shipman, L. L.; Thurnauer, M. C.; Wasielewski, M. R. *Annu. Rev. Biophys. Bioeng.* **1978**, *7*, 393−434.
(5) Fujita, I.; Davis, M. S.; Fajer, J. *J. Am. Chem. Soc.* **1978**, *100*, 6280−6282.
(6) Fajer, J.; Brune, D. C.; Davis, M. S.; Forman, A.; Spaulding, L. D. *Proc. Natl. Acad. Sci. U.S.A.* **1975**, *72*, 4956−4960.
(7) Borg, D. C.; Fajer, J.; Felton, R. H.; Dolphin, D. *Proc. Nat. Acad. Sci. U. S.* **1970**, *67*, 813−820.
(8) Fabian, J.; Nakazumi, H.; Matsuoka, M. *Chem. Rev.* **1992**, *92*, 1197−1226.
(9) Inoue, S.; Aso, Y.; Otsubo, T. *Chem. Commun.* **1997**, 1105−1106.
(10) Rurack, K.; Bricks, J. L.; Reck, G.; Radeglia, R.; Resch-Genger, U. *J. Phys. Chem. A* **2000**, *104*, 3087−3109.
(11) Bai, J.-F.; Zuo, J.-L.; Tan, W.-L.; Ji, W.; Chen, Z.; Fun, H.-K.; Chinnakali, K.; Razak, I. A.; You, X.-Z.; Che, C.-M. *J. Mater. Chem.* **1999**, *9*, 2419−2423.
(12) Holtrup, F. O.; Muller, G. R. J.; Quante, H.; De Feyter, S.; De Schryver, F. C.; Mullen, K. *Chem. Eur. J.* **1997**, *3*, 219−225.
(13) Langhals, H.; Schonmann, G.; Feiler, L. *Tetrahedron Lett.* **1995**, *36*, 6423−6424.
(14) Geerts, Y.; Quante, H.; Platz, H.; Mahrt, R.; Hopmeier, M.; Bohm, A.; Mullen, K. *J. Mater. Chem.* **1998**, *8*, 2357−2369.
(15) Langhals, H.; Sprenger, S.; Brandherm, M.-T. *Liebigs. Ann.* **1995**.
(16) Quante, H.; Geerts, Y.; Mullen, K. *Chem. Mater.* **1997**, *9*, 495−500.
(17) Langhals, H.; Jaschke, H.; Ring, U.; von Unold, P. *Angew. Chem., Int. Ed.* **1999**, *38*, 201−203.
(18) Sakamoto, T.; Pac, C. *J. Org. Chem.* **2001**, *66*, 94−98.
(19) Fleury, L.; Zumbusch, A.; Orrit, M.; Brown, R.; Bernard, J. *J. Lumin.* **1993**, *56*, 15−28.
(20) Moener, W. E.; Plakhotnik, T.; Irngartinger, T.; Croci, M.; Palm, V.; Wild, U. P. *J. Phys. Chem.* **1994**, *98*, 7382−7389.
(21) Kummer, S.; Basche, T.; Brauchle, C. *Chem. Phys. Lett.* **1994**, *229*, 309−316.
(22) Basche, T.; Kummer, S.; Brauchle, C. *Nature* **1995**, *373*, 132−134.
(23) Kulzer, F.; Kummer, S.; Matzke, R.; Brauchle, C.; Basche, T. *Nature* **1997**, *387*, 688−691.
(24) Schlichting, P.; Duchscherer, B.; Seisenberger, G.; Basche, T.; Brauchle, C.; Mullen, K. *Chem. Eur. J.* **1999**, *5*, 2388−2395.
(25) Belfield, K. D.; Schafer, K. J.; Alexander, M. D., Jr. *Chem. Mater.* **2000**, *12*, 1184−1186.
(26) Leznoff, C. C. In *Phthalocyanines: Properties and Applications*; Leznoff, C. C., Lever, A. B. P., Eds.; VCH Wiley: 1989; Vol. 1, pp 1−54.
(27) Kadish, K. M., Smith, K. M., Guilard, R., Eds. *Synthesis and Organic Chemistry*; Academic Press: 2000; Vol. 1.
(28) Zhao, Y.; Wasielewski, M. R. *Tetrahedron Lett.* **1999**, *40*, 7047−7050.
(29) Lee, S. K.; Zu, Y.; Herrmann, A.; Geerts, Y.; Mullen, K.; Bard, A. J. *J. Am. Chem. Soc.* **1999**, *121*, 3513−3520.
(30) Langhals, H.; Kirner, S. *Eur. J. Org. Chem.* **2000**, 365−380.
(31) Lukas, A. S.; Miller, S. E.; Wasielewski, M. R. *J. Phys. Chem. B* **2000**, *104*, 931−940.
(32) Greenfield, S. R.; Wasielewski, M. R. *Opt. Lett.* **1995**, *20*, 1394−1396.
(33) Gosztola, D.; Niemczyk, M. P.; Svec, W.; Lukas, A. S.; Wasielewski, M. R. *J. Phys. Chem. A* **2000**, *104*, 6545−6551.
(34) Karki, L.; Lu, H. P.; Hupp, J. T. *J. Phys. Chem.* **1996**, *100*, 15637.
(35) Karki, L.; Hupp, J. T. *Inorg. Chem.* **1997**, *36*, 3318−3321.
(36) Miller, S. E.; Zhao, Y.; Schaller, R.; Mulloni, V.; Just, E. W.; Johnson, R. C.; Wasielewski, M. R. *Chem. Phys.* **2002**, in press.
(37) Viehbeck, A.; Goldberg, M. J.; Kovac, C. A. *J. Electrochem. Soc.* **1990**, *137*, 1460−1466.
(38) Davis, M. S.; Forman, A.; Fajer, J. *Proc. Natl. Acad. Sci. U.S.A.* **1979**, *76*, 4170−4174.
(39) Osuka, A.; Nagata, T.; Maruyama, K.; Mataga, N.; Asahi, t.; Yamazaki, I.; Nishimura, Y. *Chem. Phys. Lett.* **1991**, *185*, 88−94.
(40) Ford, W. E.; Hiratsuka, H.; Kamat, P. V. *J. Phys. Chem.* **1989**, *93*, 6692−6696.
(41) Salbeck, J.; Kunkely, H.; Langhals, H.; Saalfrank, R. W.; Daub, J. *Chimia* **1989**, *43*, 6−9.
(42) Stewart, J. J. P. *J. Comput. Chem.* **1989**, *10*, 209−220.
(43) Stewart, J. J. P. *J. Comput. Chem.* **1989**, *10*, 221.
(44) Zerner, M. C. In *Reviews of Computational Chemistry*; Lipkowitz, K. B., Boyd, D. B., Eds.; VCH Publishing: New York, 1991; Vol. 2, p 313.
(45) Pavlopoulos, T. G.; Boyer, J. H.; Thangaraj, K. *Applied Optics* **1992**, *31*, 7089−7094.
(46) Weller, A. *Z. Phys. Chem.* **1982**, *133*, 93−98.
(47) Read, I.; Napper, A.; Zimmt, M. B.; Waldeck, D. H. *J. Phys. Chem. A* **2000**, *104*, 9385−9394.
(48) Newton, M. D. *Adv. Chem. Phys.* **1999**, *106*, 303−375.
(49) Newton, M. D.; Basilevsky, M. V.; Rostov, I. V. *Chem. Phys.* **1998**, *232*, 201−210.
(50) Basilevsky, M. V.; Rostov, I. V.; Newton, M. D. *Chem. Phys.* **1998**, *232*, 189−199.
(51) Marcus, R. A. *J. Chem. Phys.* **1956**, *24*, 966.
(52) Ivancich, A.; Artz, K.; Williams, J. C.; Allen, J. P.; Mattioli, T. A. *Biochemistry* **1998**, *37*, 11 812−11 820.
(53) Thompson, M. A.; Zerner, M. C.; Fajer, J. *J. Phys. Chem.* **1991**, *95*, 5693−5700.
(54) McDowell, L. M.; Kirmaier, C.; Holten, D. *Biochim. Biophys. Acta* **1990**, *1020*, 239−246.
(55) Jones, G., II.; Farahat, M. S.; Greenfield, S. R.; Gosztola, D. J.; Wasielewski, M. R. *Chem. Phys. Lett.* **1994**, *229*, 40−46.
(56) Greenfield, S. R.; Svec, W. A.; Gosztola, D.; Wasielewski, M. R. *J. Am. Chem. Soc.* **1996**, *118*, 6767−6777.